Proceedings of the 3rd IASME/WSEAS Int. Conf. on HEAT TRANSFER, THERMAL ENGINEERING AND ENVIRONMENT, Corfu, Greece, August 20-22, 2005 (pp214-220)

The Influence of Solar and Longwave Radiations on the Airflow in Building Spaces

B. FARHANIEH S. SATTARI
Department of Mechanical Engineering - Division of Energy Conversion
Sharif University of Technology
Tehran, P.O. Box: 11365-9567
IRAN
bifa@sharif.edu

Abstract: - The airflow and thermal gain in building spaces are influenced by solar (shortwave) radiation, the environmental longwave radiation and the radiation of the internal walls of the building considered as gray bodies at different temperatures. In this paper an integrated model includes the influence of the above radiations is developed for simulation of the airflow in building spaces. For this purpose, two modeling approaches are used, the zonal network method for modelling of the building segments and the Computational Fluid Dynamics (CFD) solution for modelling of the inner airflow. A synchronize solution process is also used for the building and CFD equation-sets.

Key-Words: Energy Simulation - Integrated Modelling - CFD - Radiation - Solar – Longwave

1 Introduction

The building sector plays a significant role in global energy consumption. Since energy production is extensively based on using fossil fuels, the building sector has a clear connection to environmental issues. These environmental and economical reasons increase the pressure to design and build better residential and commercial buildings in the future. To this end, more research is needed to better understand the behavior of buildings, and particularly to quantify the interaction between indoor air quality and energy consumption.

Energy simulation and CFD provide important and complementary information for building energy and indoor environment design. In recent years the synchronized solution of the existent building simulation and CFD programs to achieve more accurate results is increased. Bartak et al. [1], Morrison [2, 3] and Hensen [4] have investigated on the integrated building and airflow simulations. A coupled energy simulation and CFD simulation can eliminate many assumptions employed in the separate energy simulation and CFD computations and thus provide more accurate results [5].

The gain of energy from the sun has major effects on thermal behavior of airflow in the building. Many researchers have investigated to calculate the gain of solar radiation which receives at earth's surface [6-8]. The total radiation incident on an exposed surface with arbitrary inclination and azimuth angles has three components, direct solar beam, ground reflected and sky diffuse. In order to calculate of these values some data on local solar time, solar position and climate modeling are necessary. Bring and et al. [9] have gathered some different models for building indoor climate and energy simulation. Atheanassouli and Massouros [10] obtained an explicit relation for the thermal flux from the environment to an opaque external wall.

Hong et al. [11] have reviewed the state-of-the-art on the development and application of computer-aided building simulation. They have provided also some information sources to the building simulation community.

In this paper an integrated model is developed for simulation of the airflow in building spaces. The influence of the solar and longwave radiations on airflow is investigated using this developed model. For this purpose a 2D building space surrounded with multi-layer walls and a window is considered (Fig.1). Since different numerical methods are employed in walls and CFD modelings, we employed an iterative procedure in order to achieve the convergence and stability in corresponding solution.

2 Airflow (CFD) Modelling

CFD has the potential to predict the details of airflow and temperature fields within particular zone by solving the flow's governing equations. In the last two decades, CFD has been successfully applied to the indoor airflow analysis [5].

2.1 Governing Equations

CFD solves the partial differential flow governing equations for mass, momentum, and energy conservation in an indoor space. The two-dimensional steady-state Navier-Stocks governing equations on airflow in conservative form can be written as follows

$$F_{,x}+G_{,y}=R_{,x}+T_{,y}+B \tag{1}$$

Where a comma represents differentiation with respect to coordinates and the convection flux, diffusion flux and body force vectors are as

$$\begin{aligned} F&=(\rho u,\ \rho u^2+p,\ \rho uv,\ \rho uh)\\ G&=(\rho v,\ \rho uv,\ \rho v^2+p,\ \rho vh)\\ R&=(0,\ \tau_{xx},\ \tau_{xy},\ \sigma_{xx})\\ T&=(0,\ \tau_{yx},\ \tau_{yy},\ \sigma_{yy})\\ B&=(0,\ \rho_\circ g_x\beta(T_i-T_\circ),\ \rho_\circ g_y\beta(T_i-T_\circ),\ 0) \end{aligned} \tag{2}$$

where the viscous stress tensor given by

$$\sigma_{xx}=u\tau_{xx}+v\tau_{xy}+kT_{,x} \quad \sigma_{yy}=u\tau_{yx}+v\tau_{yy}+kT_{,y}$$

$$\tau_{xx}=\tfrac{2}{3}\mu\left(2u_{,x}-v_{,y}\right) \qquad \tau_{yy}=\tfrac{2}{3}\mu\left(2v_{,y}-u_{,x}\right)$$

$$\tau_{xy}=\tau_{yx}=\mu(u_{,y}+v_{,x}) \tag{3}$$

We introduce the following dimensionless variables

$$u^*=u/U_0 \quad v^*=v/U_0 \quad p^*=p/(\rho_0 U_0^{\,2})$$

$$T^*=(T-T_c)/(T_H-T_c) \quad \rho^*=\rho/\rho_0 \tag{4}$$

The independent parameters are

$$U_0=\alpha_0/L_0=k_0/(\rho_0 c_p L_0) \quad T_0=\tfrac{1}{4}(T_1+T_2+T_3+T_4)$$

$$Ra=\rho g\beta\left(T_H-T_C\right)L^3/k_0\nu_0 \quad \alpha_0=k_0/\rho_0 c_p \tag{5}$$

Also, in this paper we consider the following constant parameters to present the results

$$L=L_0=1 \quad Pr=\mu_0 c_p/k_0=0.71 \quad c_p=1004.5$$

$$k=k_0=const. \quad \mu=\mu_0=const. \tag{6}$$

Therefore nondimensionalized governing equations after dropping the asterisks in the dimensionless physical variables are

$$\begin{aligned} &u_{,x}+v_{,y}=0\\ &(uu)_{,x}+(uv)_{,y}=-P_{,x}+Pr(u_{,xx}+u_{,yy})\\ &(uv)_{,x}+(vv)_{,y}=-P_{,y}+Pr\,(v_{,xx}+v_{,yy})+Ra\,Pr\,T\\ &(uT)_{,x}+(vT)_{,y}=T_{,xx}+T_{,yy} \end{aligned} \tag{7}$$

The governing equations (7) are subject to the Boussinesq approximation. Researchers have defined a relatively temperature difference parameter ε as the difference between the hot and cold wall temperatures divided by their sum, i.e. $\varepsilon=(T_H-T_C)/(T_H+T_C)$ [12]. For small temperature-difference, $\varepsilon<0.2$, the Boussinesq approximation is valid. In fluid dynamics, the Boussinesq approximation is used in the field of buoyancy-driven flow. It states that density differences are sufficiently small to be neglected, except where they appear in terms multiplied by *g*, the acceleration due to gravity.

In order to CFD solution of the airflow we discretized the indoor two-dimensional solution domain, figure 1, using a staggered grid technique. Also, SIMPLE (Semi-Implicit Method for Pressure-Linked Equations) algorithm [13] is used to solve the discretized equations.

3 Modeling of Multi-Layer Wall

3.1 Nodal Network Modelling

The nodal network method is a well adapted model in building energy simulation. In this method, the building are treated as a network of nodes representing various parts such as rooms, parts of rooms and system components, with inter-nodal connections representing the distributed flow paths [4, 14].

Integration of the network method with building energy simulation is an established technology and today commonly used in various applications. The reasons for this are: 1) The information demands of the energy conservation formulations can be directly satisfied. 2) The technique can be readily applied to combined multi-zone. 3) The number of nodes involved will be considerably less than that required in a CFD approach and so the additional CPU time is minimized.

3.2 Heat Transfer Simulation

In this section heat transfer simulation based on the nodal network approach is presented. In nodal network method the solid parts of construction of 2D domain Fig.1 is replaced by some nodes (for example Fig.2). These nodes are connected to each other by one-dimensional heat transfer elements. Forms of heat transfer in energy analysis are shortwave and longwave radiations, heat convection and heat conduction through building elements such as walls and window. A heat balance method is selected for the evaluation of temperature distribution in solid parts due to conduction. In such a method, for a physical system I with volume δV_I which has conditionally heat exchange with region J, the heat balance consideration yields

$$\begin{aligned} &\rho_I(\xi)C_I(\xi)\delta V_I(\xi)\left(T_I^{\,t+\delta t}-T_I^{\,t}\right)/\delta t\\ &\qquad=k_I\left(T_J^{\,\xi}-T_I^{\,\xi}\right)+q_I^{\,\xi} \end{aligned} \tag{8}$$

ξ is the time. For $\xi=t$ equation (8) gives the explicit formulations and for $\xi=t+\Delta t$ it gives the

fully implicit formulation. Also, the Crank-Nicolson formulation can be obtained as a summation of both schemes. So, in (8) q_I is the heat generation within region I. The value of q_I depends on the position of I. Total heat generation for a node located on the exterior wall surface is

$$q_{EWS}=q_{abs}+q_{lw-sky}+q_{lw-ground} \tag{9}$$

where $q_{abs}=\alpha_m(I_{Dir}+I_{Diff})$ is the total absorbed solar radiation. I_{Dir} is direct radiation and I_{diff} is diffuse radiation on wall. q_{lw-sky} and $q_{lw-ground}$ are the longwave radiation between the exterior surfaces with the sky and the ground, respectively. These values calculate from the subsequent equations

$$q_{lw-sky}=F_{ws}\varepsilon_{wall}\left(T_{sky}^4-T_{wall}^4\right)$$
$$q_{lw-ground}=F_{wg}\varepsilon_{wall}\left(T_{ground}^4-T_{wall}^4\right) \tag{10}$$

where F_{ws} is the view factor between the sky and the wall (or window) and F_{wg} is the view factor between the ground and the wall (or window).

Now based on equation (8) and Crank-Nicolon scheme we establish the interrelated equations to representing the discrete nodal network. Figure 2 shows a two dimensional solid construction with two layers. A simple nodal model is imposed on conductive heat transfer. In this model the solid surface is replaced by some nodes where each node represents the different parts of the surface as follows.

a) Nodes that represent the energy balance of regions located in solid surface such as node 3 and node 5. For such nodes we have

$$\begin{aligned}\left(2+2\Psi_i+2\Phi_i\right)T_I^{t+\Delta t}=&(2-2\Psi_i-2\Phi_i)T_I^t+\\ &\Psi_i T_{I+1}^t+\Psi_i T_{I+1}^{t+\Delta t}+\Psi_i T_{I-1}^t+\Psi_i T_{I-1}^{t+\Delta t}\\ &+\Phi_i T_{J+1}^t+\Phi_i T_{J+1}^{t+\Delta t}+\Phi_i T_{J-1}^t+\Phi_i T_{J-1}^{t+\Delta t}\end{aligned} \tag{11}$$

where $\Psi_i=k_i\Delta t/\rho_i C_i\Delta x_i^2$, $\Phi_i=k_i\Delta t/\rho_i C_i\Delta y_i^2$ and subscript $i\left(=A,B,...\right)$ stand for each layer. Equation (11) defines the transient conduction node case and is equivalent to a Crank-Nicolson difference formulation.

b) Nodes that represent the energy balance at boundary surface of two separate layers, such as node 4. For such nodes Crank-Nicolson difference formulation yields

$$\begin{aligned}\left(2+\bar{\Psi}_A+\bar{\Psi}_B+\bar{\Phi}_A+\bar{\Phi}_B\right)T_I^{t+\Delta t}&\\ =(2-\bar{\Psi}_A-\bar{\Psi}_B-\bar{\Phi}_A-\bar{\Phi}_B)T_I^t&\\ +\bar{\Psi}_A T_{I-1}^t+\bar{\Psi}_B T_{I+1}^t+\bar{\Phi}_A T_{J-1}^t+\bar{\Phi}_B T_{J+1}^t&\end{aligned} \tag{12}$$

where

$$\begin{aligned}&\bar{\Psi}_A=2k_A\Delta t/\mathrm{P}\Delta x^2 \quad \bar{\Psi}_B=2k_B\Delta t/\mathrm{P}\Delta x^2\\ &\bar{\Phi}_A=2k_A\Delta t/\mathrm{P}\Delta y^2 \quad \bar{\Phi}_B=2k_B\Delta t/\mathrm{P}\Delta y^2\\ &\mathrm{P}=\left(\rho_A C_A+\rho_B C_B\right)\end{aligned} \tag{13}$$

c) Nodes that represent the energy balance at bounding surface of external wall or window, such as node 6. If node I is suited at interface of a fluid volume and adjacent material layer then Crank-Nicolson difference formulation yields

$$\begin{aligned}&(1+\Psi+\Phi+\mathrm{H}_x+\mathrm{H}_y)T_I^{t+\Delta t}=(1-\Psi-\mathrm{H}_x-\Phi-\mathrm{H}_y)T_I^t\\ &+\tfrac{1}{2}(\mathrm{H}_x(T_{I-1}^t+T_{I-1}^{t+\Delta t})+\mathrm{H}_y(T_{J-1}^t+T_{J-1}^{t+\Delta t}))\\ &+\Psi(T_{I+1}^t+T_{I+1}^{t+\Delta t})+\Phi(T_{J+1}^t+T_{J+1}^{t+\Delta t})+\mathrm{I}_{ss}(T_{sky}^4-T_I^{t\,4})\\ &+\mathrm{I}_{sg}(T_{ground}^4-T_I^{t\,4})+\mathrm{I}_{abs}\end{aligned} \tag{14}$$

where

$$\begin{aligned}&\mathrm{H}_x=h_c\Delta t/\rho C\Delta x \quad \mathrm{H}_y=h_c\Delta t/\rho C\Delta y\\ &\mathrm{I}_{ss}=F_{ws}\varepsilon_{wall}\Delta t/\rho C\Delta x \quad \mathrm{I}_{sg}=F_{wg}\varepsilon_{wall}\Delta t/\rho C\Delta x\\ &\mathrm{I}_{abs}=q_{abs}\Delta t/\rho C\end{aligned} \tag{15}$$

d) Nodes that represent the energy balance at bounding surface of internal wall or window, such as node 2. For this node the Crank-Nicolson difference formulation yields

$$\begin{aligned}&(1+\Psi+\Phi+\mathrm{H}_x+\mathrm{H}_y)T_I^{t+\Delta t}=(1-\Psi-\mathrm{H}_x-\Phi-\mathrm{H}_y)T_I^t\\ &+\tfrac{1}{2}(\mathrm{H}_x(T_{I-1}^t+T_{I-1}^{t+\Delta t})+\mathrm{H}_y(T_{J-1}^t+T_{J-1}^{t+\Delta t}))\\ &+\Psi(T_{I+1}^t+T_{I+1}^{t+\Delta t})+\Phi(T_{J+1}^t+T_{J+1}^{t+\Delta t})\\ &+\mathrm{I}_{w_iw_j}(T_{w_j}^4-T_I^{t\,4})\end{aligned} \tag{16}$$

where

$$\mathrm{I}_{w_iw_j}=F_{w_iw_j}\varepsilon_{w_i}(1-\varepsilon_{w_j})\sigma\Delta t/\rho C \tag{17}$$

where $i,j=1..4$ insisted of the four interior wall surfaces. The radiation emitted by each surface will be totally absorbed after multiple reflections, in the process, redistributed [14]. In practice the recursive process continue until the reflected flux is reduced to insignificance. In this work a three recursive steps is considered for modeling the exchange of longwave radiation between internal considered gray surfaces.

In this section, the energy conservation equations for a composite solid surface are derived. To solution these set of equations, the system of equations expressed in matrix notation as $\mathbf{AT}_{n+1}=\mathbf{BT}_n$, where $\mathbf{A}$ and $\mathbf{B}$ established a matrix with future and the present time coefficient, respectively. $\mathbf{T}$ is vector of nodal temperature, $n+1$ and n refer to future and the present time, respectively. Initial conditions are $\mathbf{T}(0)=\mathbf{T}_0$. Also, a specially adapted solver is used to minimize the computational effort.

4 Synchronize Solution of Equations

To synchronize solution of building and airflow, a coupled simulation method is used. In this method two separate matrix equations, one for solid surfaces in nodal network energy simulation and another for indoor airflow in CFD, are solved using an iterative procedure. The iterative solution is provided the converged and stable solution. In order to reduce the computational efforts in synchronized solution process, we used separate solution algorithms for each method based on sparse and TDMA matrix theories.

The interior surface convective heat flux and surface temperature are linked the nodal network energy simulation and CFD methods. The convected heat from the indoor environment to solid surface is equivalent to:

$$q_c = h_c (T_{air} - T_{wall}) \quad (18)$$

where h_c is surface-averaged convective heat transfer coefficient. And $(T_{air} - T_{wall})$ is the difference between the air and the solid surface temperatures. In this study an improved convection coefficient which presented by Alamdary et al. [15] is used as follows:

$$h_c = (a^m L^{-pm} (T_{air} - T_{wall})^{pm} + b^m (T_{air} - T_{wall})^{qm})^{1/m} \quad (19)$$

where for buoyancy-driven convection over vertical surfaces:

$$a=1.5,\ b=1.23,\ p=1/4,\ q=1/3,\ m=6 \quad (20)$$

and for convection on horizontal surfaces:

$$a=1.4,\ b=1.63,\ p=1/4,\ q=1/3,\ m=6 \quad (21)$$

From these equations it is found that h_c is itself a function of the temperature difference $(T_{air} - T_{wall})$ and must be updated during the iterative solution.

5 Applications

5.1 Verification of the CFD Modeling

In this example a 2D rectangular domain as illustrated in Fig.3 is considered. The left and right walls are maintained at temperature of T_H and T_C, respectively, where $T_H - T_C = 10^{\circ}C$. The top and bottom walls are insulated. This problem has studied as a benchmark to verification of the results by previous researchers [12, 16]. Fig.4 shows the variation of the Nusselt number on vertical walls. On these walls the Nusselt number is defined as $Nu_y = \frac{L k}{k_0 (T_H - T_C)} \left.\frac{dT}{dx}\right|_{wall}$.

Figs 5 and 6 show the variations in the velocity profiles *u* and *v* along the horizontal and vertical lines passing through the geometrical center of domain. The constant temperature lines and flow patterns shown in Figs 7 and 8 for Raleigh number=10^5, respectively. The analysis of the results indicated that there are good agreements between the present solution and the benchmark solution [11].

5.2 Influence of Radiations on the Airflow in Building Spaces

The 2D airflow in the building domain Fig. 1 is considered in this problem. It is assumed that the construction of the solid surface is bricks in middle, plaster layers on both sides and the columns in the corners with properties of Table 1. The indoor gas also is assumed to be in the initial constant temperature and four exterior (solid) surfaces are in various temperatures. In order to study the effects of solar and environmental radiations on airflow in the building spaces, this problem has solved in two conditions: I) without taking into account any radiations, II) considering the solar, environmental and inner walls radiations in the solution.

An iterative procedure with 12 iterations is used to solution this coupled domain. These numbers of iterations is provided the converged and stable solution with Error= 5×10^{-4}. In Figs 9 and 10 we have compared the results from the two addressed conditions for the velocity profiles *u* and *v* along the horizontal and vertical lines passing through the geometrical center of indoor domain. The flow patterns from the two conditions also are shown in Figs 11 and 12 for Raleigh number $=10^5$. Analysis of these results indicated that, they have physically meaningful. So, the radiations have significant effects on the airflow in building spaces.

6 Conclusion

The influence of solar energy as well as the environmental and internal wall longwave radiations is investigated on the airflow in building spaces using a developed integrated model. For this purpose, the nodal network method as a well adapted model in building energy simulation together with the CFD method are coupled used to modeling a 2D indoor airflow surrounded with composite walls. An iterative procedure is used to synchronize solution of the different mathematical and numerical methods, which are employed in energy simulation and CFD modeling. From the results it is noted that the influence of the radiations on the airflow in building space are significant. Indeed the solar radiation increased the temperature of the external as well as the internal walls consequently increased their emission as gray bodies are.

NOMENCLATURE

h	enthalpy
g	gravity acceleration
p	pressure
k	thermal conductivity coefficient
u, v	velocity components
x, y	coordinates directions
T	temperature
T_i	$i=1\text{-}4$, four walls temperature
T_0	initially (reference) temperature
T_H	hot wall temperature
T_C	cold wall temperature
Pr	Prandtl number
Re	Reynolds number
L	wall dimensions
c_p	specific heat at constant pressure
C	specific heat capacity
t	time
h_c	thermal convection coefficient
q	heat flux
ρ	density
β	coefficient of volume expansion
ε	temperature-difference parameter
ε_{wall}	emissivity of the wall surface
α	thermal diffusivity
α_m	absorptivity of the material
τ_{ij}, σ_{ii}	viscous stress tensor component
σ	Stefan-Boltzman constant
μ	dynamic viscosity
ν	kinematic viscosity
ξ	a time parameter

References:

[1] Bartaka M. et al., *Integrating CFD and building simulation*, Building and Environment 2002; (37) : 865 – 871.

[2] Morrison IB., *An algorithm for calculating convection coefficients for internal building surfaces for the case of mixed flow in rooms*, Energy and Buildings 2001; (33) : 351-361.

[3] Morrison IB., *The adaptive conflation of computational fluid dynamics with whole-building thermal simulation*, Energy and Buildings 2002; (34) : 857–871.

[4] Hensen JLM., *Integrated building (and) airflow simulation: an overview* In: 9th International Conference on Computing in Civil and Building Engineering, Taiwan, 2002.

[5] Zhai Z. and Chen Q., *Solution characters of iterative coupling between energy simulation and CFD programs*, Energy and Buildings 2003; (35) : 493-505.

[6] Kambezidis HD., Psiloglou BE. and Gueymard C., *Measurements and models for total solar irradiance on inclined surface in Athens, Greece*, Solar Energy, 1994; (53) : 177-185.

[7] Ahmad F. and Ulfat I., *Empirical models for the correlation of monthly average daily global solar radiation with hours of sunshine on a horizontal surface at Karachi, Pakistan,* Turk J Phys, 2004; (28) : 301-307.

[8] Bhandari MS. and Bansal NK., *Solar heat gain factors and heat loss coefficients for passive heating concepts,* Solar Energy, 1994; (53) : 199-208.

[9] Bring A., Sahlin P. and Vuolle M., *Models for Building Indoor Climate and Energy Simulation*, A Report of IEA SHC Task 22, Building Energy Analysis Tools, Subtask B, Ver. 1.0, Sep. 1999, Stockholm, Sweden.

[10] Atheanassouli G. and Massouros G., *The influence of solar and longwave radiations on the thermal gain of a room with opaque external wall,* Solar Energy, 1983; (30) : 161-170.

[11] Hong T., Chou SK. and Bong TY., *Building simulation: an overview of developments and information sources,* Building and Environment 2000; (35) : 347-361.

[12] Chenoweth DR. and Paolucci S., *Natural convection in an enclosed vertical air layer with large horizontal temperature differences*, Journal of Fluid Mechanics 1986; (169) : 173-210.

[13] Patankar SV., *Numerical heat transfer and fluid flow*, second edition, Hemisphere, New York, 1996.

[14] Clarke JA., *Energy simulation in building design*, second edition, Butterworth-Heinemann, 2001.

[15] Alamdari F. and Hammond GP., *Improved for buoyancy-driven convection in rooms, Building Services*, Engineering Research and Technology 1982; (4) : 106-12.

[16] Ismail KAR. and Scalon VL., *A finite element free convection model for the side wall heated cavity*, International Journal of Heat and Mass Transfer 2000; (43) : 1373-1389.

Table1- Properties of the composite wall components

	k $W/m^{\circ}C$	C $J/kg^{\circ}C$	ρ kg/m^3	*Width* *Cm*
Interior Plaster	0.51	960	1120	1.0
Brick	0.75	840	1300	20
Exterior Plaster	0.79	1000	1330	2.0
Column	0.32	840	1050	

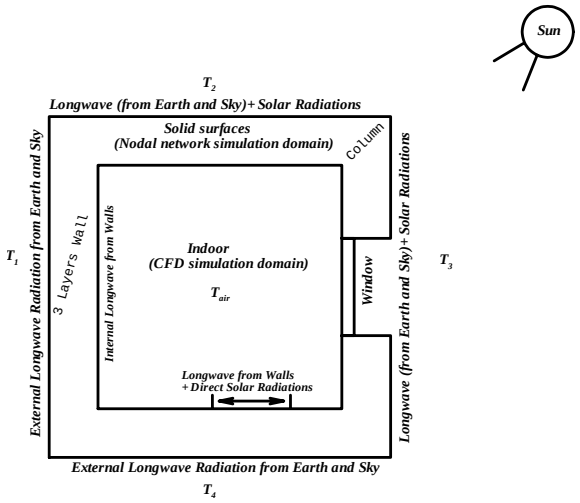

Fig.1- 2D solution domain (main problem)

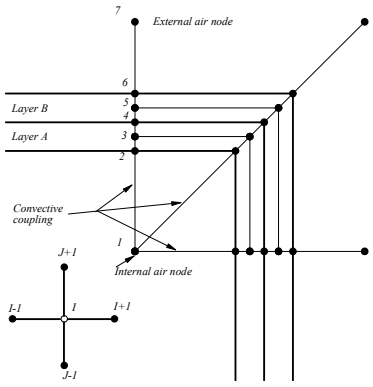

Fig.2- A sample for nodal network discretization

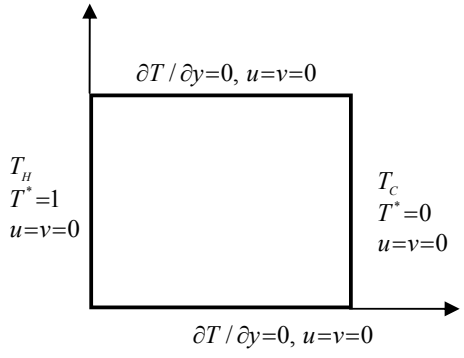

Fig.3- Layout of problem 1

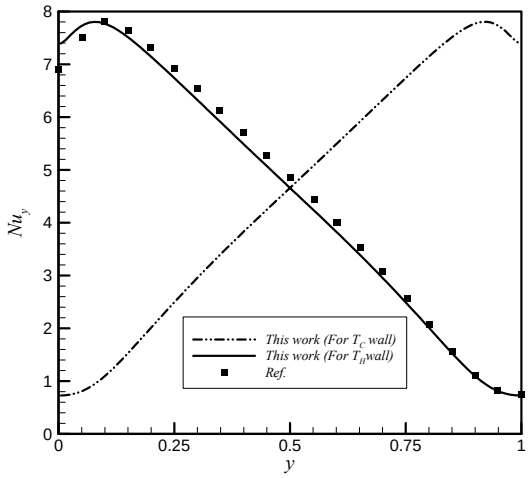

Fig.4- Nusselt numbers distribution

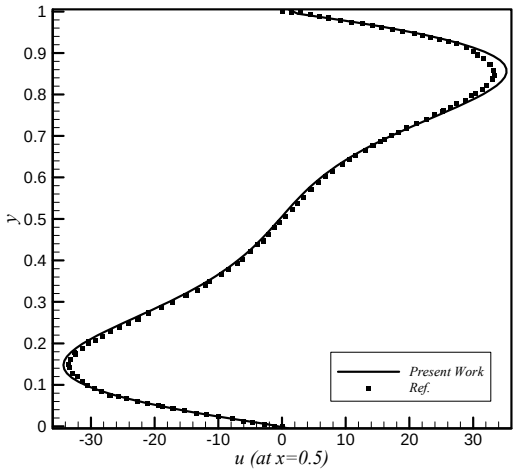

Fig.5- Profile of the horizontal velocity component

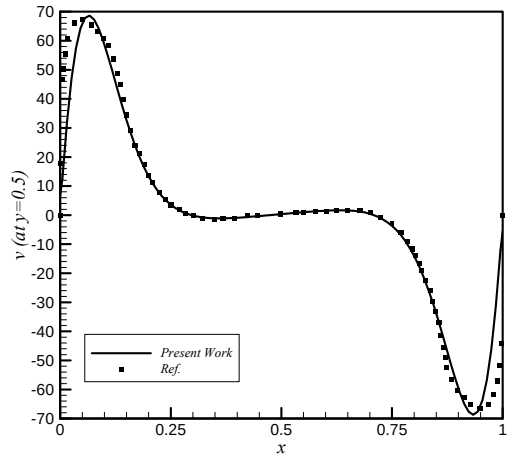

Fig.6- Profile of the vertical velocity component

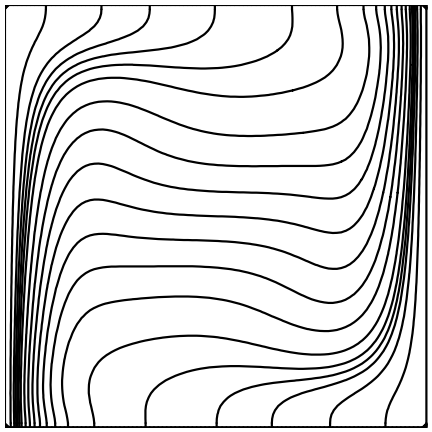

Fig.7- Constant temperature lines in Fig.1 domain

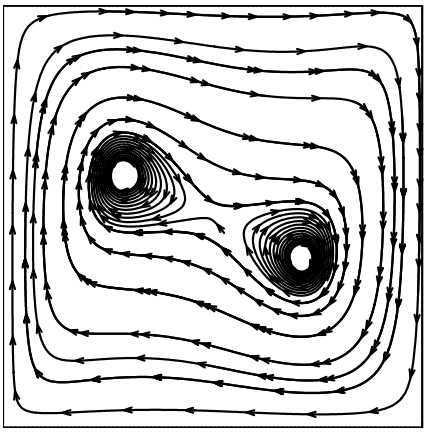

Fig.8- Flow pattern in Fig.1 domain

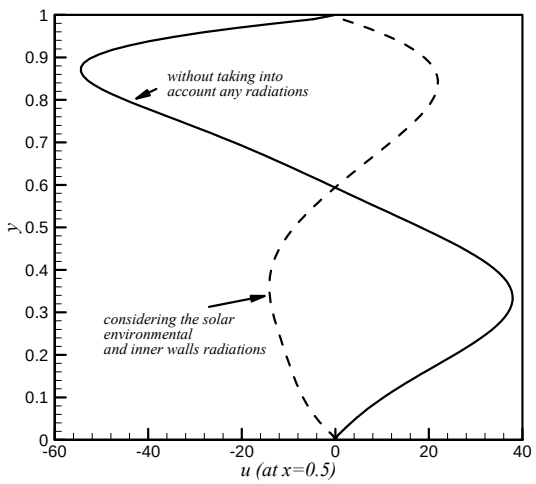

Fig.9- Comparison of the horizontal velocity components

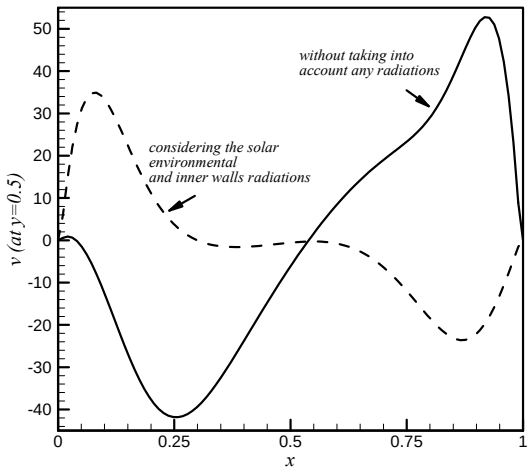

Fig.10- Comparison of the vertical velocity components

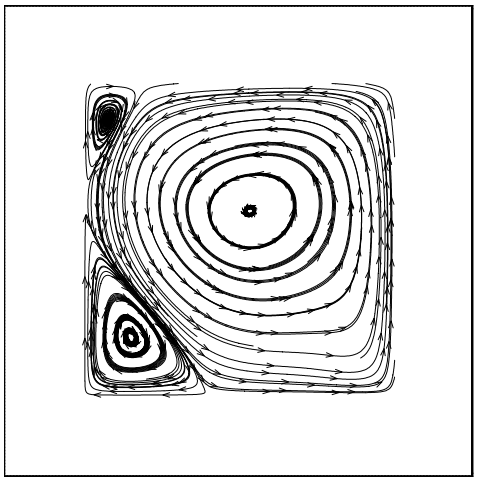

Fig.11- Indoor flow pattern (without taking into account any radiations)

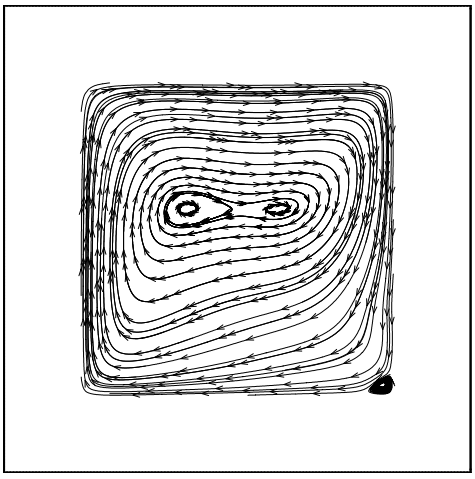

Fig.12- Indoor flow pattern (with considering radiations)